



Disrupted small-world white matter networks in patients with major depression and recent suicide plans or attempts

Huiru Li^{1,2} · Huawei Zhang^{1,5} · Kun Qin^{1,6} · Li Yin³ · Ziqi Chen^{1,5} · Feifei Zhang^{1,6} · Baolin Wu^{1,6} · Taolin Chen^{1,6} · John A. Sweeney^{1,4} · Qiyong Gong^{1,5,6} · Zhiyun Jia^{5,6,7}

Accepted: 19 February 2024 / Published online: 26 February 2024

© The Author(s), under exclusive licence to Springer Science+Business Media, LLC, part of Springer Nature 2024

Abstract

Suicide is a major concern for health, and depression is an established proximal risk factor for suicide. This study aimed to investigate white matter features associated with suicide. We constructed white matter structural networks by deterministic tractography via diffusion tensor imaging in 51 healthy controls, 47 depressed patients without suicide plans or attempts and 56 depressed patients with suicide plans or attempts. Then, graph theory analysis was used to measure global and nodal network properties. We found that local efficiency was decreased and path length was increased in suicidal depressed patients compared to healthy controls and non-suicidal depressed patients; moreover, the clustering coefficient was decreased in depressed patients compared to healthy controls; and the global efficiency and normalized characteristic path length was increased in suicidal depressed patients compared to healthy controls. Similarly, compared with those in non-suicidal depressed patients, nodal efficiency in the thalamus, caudate, medial orbitofrontal cortex, hippocampus, olfactory cortex, supplementary motor area and Rolandic operculum was decreased. In summary, compared with those of non-suicidal depressed patients, the structural connectome of suicidal depressed patients exhibited weakened integration and segregation and decreased nodal efficiency in the fronto-limbic-basal ganglia-thalamic circuitry. These alterations in the structural networks of depressed suicidal brains provide insights into the underlying neurobiology of brain features associated with suicide.

Keywords Suicide · Major depressive disorder · Connectome · Graph theory · Diffusion tensor imaging

Huiru Li MD, Huawei Zhang MD and Kun Qin MD contributed equally to this work.

✉ Qiyong Gong
qiyonggong@hmrrc.org.cn

✉ Zhiyun Jia
jjazhiyun@wchscu.edu.cn

¹ Huaxi MR Research Center (HMRRRC), Department of Radiology, West China Hospital of Sichuan University, Chengdu 610041, China

² First Affiliated Hospital of Kunming Medical University, Kunming, Yunnan 650032, China

³ Department of Psychiatry, West China Hospital of Sichuan University, Chengdu 610041, China

⁴ Department of Psychiatry and Behavioral Neuroscience, University of Cincinnati, Cincinnati, USA

⁵ Research Unit of Psychoradiology, Chinese Academy of Medical Sciences, Chengdu 610041, China

⁶ Functional and Molecular Imaging Key Laboratory of Sichuan University, Chengdu 610041, China

⁷ Department of Nuclear Medicine, West China Hospital, Sichuan University, No. 37 GuoXue Xiang, Chengdu, Sichuan 610041, PR China

Introduction

Suicide has taken a tremendous toll on global public health, with an annual global age-standardized suicide rate of 11.4 per 100,000 people, which translates to approximately 800,000 people dying by suicide every year. Despite intensified research on suicide and suicidal behavior in the past decade, the neurobiological basis of suicide has not been fully elucidated. Retrospective, psychological autopsies and/or medical reports have shown that approximately 90% of individuals who die by suicide have an identifiable psychiatric disorder before death, predominantly depression (Arsenault-Lapierre et al., 2004). Major depressive episodes, major depressive disorder (MDD) or bipolar disorder (BP), account for most suicide deaths (Hawton & van Heeringen, 2009).

In recent years, investigators have documented multiple regional structural and functional brain abnormalities in MDD patients associated with suicide ideation or attempts, including alterations in the prefrontal cortex (PFC) (Ding et al., 2015; Monkul et al., 2007; Olvet et al., 2014), limbic regions (Colle et al., 2015; Jia et al., 2014; Myung et al., 2016), and the parietal (Chen et al., 2015) and temporal lobes (Kang et al., 2017; Peng et al., 2014). While most of this structural and functional evidence comes from MRI studies, examinations of postmortem brain tissue have reported altered neurochemistry in the ventral PFC, including a reduction in serotonin transporter sites in suicide victims (Arango et al., 2002). Disturbances within these brain regions can lead to dysfunction in more widely distributed brain networks, including the ability to coordinate activity across brain regions. This pattern of disruptions within fronto-limbic-thalamic networks in those with suicide plans or attempts may disrupt emotional functions and behavioral control and may be directly related to suicide risk (Jia et al., 2010, 2014; Johnston et al., 2017; Kang et al., 2017; Wang et al., 2020).

Several studies have investigated the suicidal brain at the level of network connectivity. Previous resting-state network studies have reported that depressed suicidal brains exhibit decreased connectivity within the default mode network (DMN), salience network (SN) and orbitofrontal-thalamic network compared with non-suicidal controls (Cao et al., 2016; Chase et al., 2017; Jung et al., 2020; Kim et al., 2017). Additionally, a graph theoretical analysis using fMRI reported slightly better integration and worse segregation of the brain network in depressed suicidal brains than in healthy participants (Weng et al., 2019). The function and structure of the brain are tightly interconnected. Although functional interaction is constrained by the anatomy of the brain (Honey et al., 2009), several researchers have suggested that the structure and function of the brain are likely

to interact bidirectionally (Sui et al., 2014; Vanes & Dolan, 2021). Structural network analysis helps us to understand the fundamental architecture of interregional connections, which differs from the information revealed by functional networks at the brain network level (Bullmore & Sporns, 2009; Myung et al., 2016). Some studies have explored the WM structure in depressed suicidal patients. Compared with non-suicidal depressed patients and healthy controls, suicide attempters with MDD exhibited reduced fiber connectivity in the anterior limb of the internal capsule and projections to the medial frontal cortex and thalamus (Jia et al., 2014). Reduced frontal-subcortical WM connectivity in MDD patients with suicidal ideation has been related to betweenness centrality network measures in this subnetwork (Myung et al., 2016). Thus, available evidence suggests that altered white matter in the fronto-limbic-thalamic circuitry is associated with suicide in patients with MDD.

Connectomics is an analytic strategy that considers the whole brain as a set of interconnected nodes that form a whole-brain network (Hagmann et al., 2008). Diffusion tensor imaging (DTI) is an MRI-based neuroimaging method for evaluating WM that can be used to characterize the structural brain connectome (Jelescu et al., 2016). DTI-based connectomics has been used to demonstrate alterations in topological parameters of the WM structural network in many psychiatric and neurological disorders (Li et al., 2020; Myung et al., 2016; Suo et al., 2017). In the present study, we calculated graph properties of WM structural networks to identify network-level alterations in depressed patients with suicide plans or attempts versus other depressed patients and healthy controls to identify brain white matter features specifically associated with suicide risk.

Materials and methods

Participants and assessment

This study protocol was approved by the West China Hospital Clinical Trials and Biomedical Ethics Committee of Sichuan University, and written informed consent was obtained from all participants. Depressed patients were recruited from the Mental Health Center, West China Hospital, Sichuan University. Diagnostic and symptom assessments were performed by two experienced clinicians on the day of scanning. Depressed patients were diagnosed using the Structured Clinical Interview for DSM-4 (SCID). Clinical symptoms in depressed patients were assessed with the 17-item Hamilton Depression Rating Scale (HAM-D-17) (Hamilton, 1960) and the Hamilton Anxiety Rating Scale (HAMA) (Hamilton, 1959). Patients who had a total HAM-D ≥ 18 were defined as patients with major depressive

disorder (MDD). MDD patients were divided into those with and without suicidality based on item 3 of the HAMD (HAMD-3). The HAMD-3 measures suicidality with a total of five levels: 0=absent, 1=feels life is not worth living, 2=wishes he were dead or any thoughts of possible death to self, 3=suicidal plan or gesture, and 4=suicidal attempt. MDD patients with HAMD-3 scores ≤ 2 were included in the group of MDD patients at lower suicide risk (DS-). The patients did not have a history of suicide plans or suicide attempts in their lifetime. MDD patients with HAMD-3 scores > 2 were included in the group of depressed patients at higher suicide risk (DS+). They had suicide intent with a specific suicide plan or a history of suicide attempt within the past week. Supplementary Table S1 lists the diagnostic instruments used to assess whether patients with depression had a history of suicide plans or attempts, and we cross-validated the diagnostic instruments with notes from the patients' parents or friends. Thus, the DS+ group included suicide attempters (SAs, patients with depression and a history of suicide attempt) and suicide planners (SPs, patients with depression and suicide intent with a specific suicide plan). Detailed information on the suicidal patients is presented in Supplementary Table S2. All participants were screened to exclude those with a history of past and present nonaffective psychosis, substance abuse disorders, neurodevelopmental disorders, or traumatic brain injury and patients with no suicidal self-injuries.

Healthy controls were recruited through local poster advertisements and screened for psychiatric or neurological diseases using the Structured Clinical Interview for DSM-4, Nonpatient Version (SCID-NP). Patients with past or current neurological or psychiatric diseases, a history of suicide attempt or head trauma with loss of consciousness, and/or first-degree relatives with known Axis I psychiatric disorders or suicidal behavior were excluded from the study.

MRI data acquisition

DTI images were acquired using a 3-Tesla MRI system (Siemens Trio) with an 8-channel phased-array head coil. DTI was performed using a single-shot echo-planar imaging sequence in 50 axial planes with 40 noncollinear diffusion sensitization gradients ($b = 1000 \text{ s/mm}^2$), as well as a reference image with no diffusion weighting (b_0 image), after using an array spatial sensitivity encoding technique to reduce susceptibility and eddy-current artifacts. The imaging parameters were as follows: repetition time msec/echo time msec, 6800/93; number of signals acquired, two; field of view, $230 \times 230 \text{ mm}^2$; acquisition matrix, 128×128 ; and 3-mm section thickness without intersection gaps.

Data preprocessing

Diffusion images were preprocessed using PANDA1.3.1, a pipeline toolbox for analyzing brain diffusion images using the FMRIB Software Library toolbox (FSL6.0.0) (Jenkinson et al., 2012) implemented in MATLAB 2013b. The main procedures were as follows: (1) The raw DICOM images were subsequently transformed into the NIfTI format using `dcm2nii`. (2) Correction for the eddy-current effect. (3) Using FSL's command BET (Brain Extraction Tool), we created a brain mask to exclude nonbrain tissues from images. (4) FA images were created by fitting a tensor model at each voxel to the image data with FSL-FDT tools (FMRIB's Diffusion Toolbox). (5) Using FMRIB's nonlinear image registration tool (FNIRT) in FSL (www.fmrib.ox.ac.uk/fsl/fnirt/index.html), the FA data of all subjects were spatially aligned to the Montreal Institute of Neurology (MNI) space with a voxel size of $2 \times 2 \times 2 \text{ mm}^3$.

Extraction of brain networks

We defined a structural connectome for each participant as comprising a collection of nodes and edges interconnecting the nodes. In detail, for each subject, the automated anatomic labeling atlas (AAL90) was used to parcellate the brain into 90 regions of interest (ROIs) (45 in each hemisphere), with each ROI defined as a node. The T1 images were co-registered with the b_0 images. Then, the co-registered T1 images were normalized to standard space, and the transformation parameters were applied to the DTI data. We used the deterministic tractography extracted from the PANDA data to construct a brain structural connectome. Using the fiber allocation continuous tracking (FACT) algorithm (Mori et al., 1999), whole-brain white matter tracts were reconstructed via DTI deterministic tractography. All white matter voxels were selected as seed voxels for fiber tracking, and deterministic fiber tracking was terminated when either the FA was < 0.2 or the turn angle was $> 35^\circ$ (Mori & van Zijl, 2002). Fiber tracts were determined by their capacity to link every pair of cortical regions using refined cortical AAL masks. The pairs of cortical regions were considered anatomically connected. We defined the average fractional anisotropy of the linking fiber tracts for each connection and obtained an average FA-weighted symmetrical anatomical 90×90 structural network matrix for each subject.

Network analyses

All graph theoretical network analyses in the present study were performed using GREYNA2.0.0 (<https://www.nitrc.org/projects/gretna>) software to investigate both the global and nodal topological properties of white matter structural

networks. A wide range of sparsity (S) thresholds was applied to each matrix to ensure that the threshold networks were suitable for small-world scalar estimation, which means that the small-world indices were larger than 1.0 (Suo et al., 2018). In the present study, we chose a threshold range of $0.05 < S < 0.34$ with an interval of 0.01 according to the rationale of previous studies (Li et al., 2020). The area under the curve (AUC) was subsequently used to measure each network metric across the sparsity parameter S . The global network measures included small-world parameters and network efficiency parameters, including the clustering coefficient (C_p), path length (L_p), normalized clustering coefficient (γ), normalized characteristic path length (λ), small-worldness scalar (σ), local efficiency (E_{loc}) and global efficiency (E_{glob}). The C_p measures the possibility of one node's neighbors being mutually connected, which reflects the local segregation together with the local efficiency. L_p is similar to global efficiency and equivalent to its inverse. E_{loc} measures the average efficiency of subgraphs across nodes. E_{glob} evaluates the efficiency of whole-network information exchange. (Achard & Bullmore, 2007). The nodal network properties included nodal degree and efficiency. The nodal degree measures the connection of the index node with all the other nodes in a graph, while nodal efficiency is defined as the ability of information to flow through a given node (Bullmore & Sporns, 2009).

Statistical analysis

Age and education duration were compared among the HC, DS-, and DS+ groups using one-way analysis of variance (ANOVA), and sex distribution was compared using the chi-square test. The continuous variables associated with the clinical data (HAMD and HAMA scores) were compared between the DS- and DS+ groups using two-sample t tests, and the categorical variables (medication use) were compared using the chi-square test. We compared the DS-group and DS+ group HAMD scores (minus the suicide item) to compare the overall severity of depression among

the MDD groups. Then, we used ANOVA to compare the area under the curve (AUC) values for each metric (including global and nodal properties) among the HC, DS- and DS+ groups, followed by the post-hoc Bonferroni correction. For nodal property analyses, a Bonferroni corrected threshold of $p < 0.05$ was applied ($p < 0.05/90$) to avoid false positives. To exclude the influence of depression severity, we performed a secondary analysis (two-sample t test) to compare both global and nodal properties between the DS+ and DS- groups using HAMD scores (minus suicide item) as a covariate. In addition, within the DS+ group, to observe heterogeneity in the DS+ group, we performed a nonparametric permutation test to compare SAs and SPs for each network metric because of the small sample sizes (Horiguchi & Uno, 2020). Pearson correlation analysis was used to assess the relationships between significant metrics and clinical symptom scores, including HAMD and HAMA scores, in the combined patient groups (DS- and DS+ groups) and in each group separately. The p values for the correlation analyses were also corrected by a Bonferroni corrected threshold of $p < 0.05$. The statistical analyses were performed with SPSS 19.0.

Results

Participants' demographic and clinical data

This study recruited 51 HCs and 103 depressed patients, including 47 DS- patients and 56 DS+ patients (including 36 SAs and 20 SPs). All participants were right-handed and native Chinese speakers (see Table 1). Sex, age, and education duration did not differ among the three groups (all $p > 0.05$). Medication status (whether or not patients were receiving psychotropic medications) also did not significantly differ between the DS- and DS+ groups ($p = 0.71$). The detailed medication information is presented in Supplementary Table S3. The DS+ group had significantly greater HAMD scores than did the DS- group ($p < 0.001$),

Table 1 Demographic and clinical characteristics of the HCs and the DS- and DS+ patients.

| Group | HC | DS- | DS+ | F/ t / χ^2 | P |
|---|--------------|---------------|---------------|-------------------|--------|
| Number (N) | 51 | 47 | 56 | - | - |
| Gender (F/M) | 33/18 | 28/19 | 38/18 | 0.769 | 0.681 |
| Age | 31.59 ± 9.29 | 28.40 ± 10.96 | 28.82 ± 10.90 | 1.395 | 0.251 |
| Education duration | 11.96 ± 2.12 | 12.40 ± 2.68 | 12.46 ± 3.73 | 0.448 | 0.640 |
| Medication-use (Yes/No) | - | 32/15 | 40/16 | 0.136 | 0.713 |
| HAMD | - | 23.72 ± 5.78 | 29.63 ± 8.61 | -3.907 | <0.001 |
| HAMD scores (minus suicide item) | - | 23.17 ± 5.67 | 26.46 ± 8.15 | -2.291 | 0.024 |
| HAMA | - | 22.57 ± 7.92 | 25.91 ± 9.68 | -1.824 | 0.071 |

The data are shown as the mean ± SD.

Abbreviations HCs: healthy controls; DS-: patient with depression and no suicide plan or attempters; DS+: patient with depression and suicide plan or attempters; SD: standard deviation; HAMD: Hamilton Depression Rating Scale; HAMA: Hamilton Anxiety Rating Scale

even when the suicide item was not considered in the analyses, although the difference was more marginal ($p=0.03$); moreover, the HAMA scores did not differ between the two groups ($p=0.07$).

Alterations in global brain network properties

All participant groups showed a small-world architecture ($\gamma > 1$, $\lambda \approx 1$, $\gamma/\lambda > 1$) at all connection densities (Fig. 1). We found differences in topological properties across participant groups. The global network characteristics that differed significantly ($p < 0.05$) included E_{glob} , E_{loc} , C_p , L_p and λ (Table 2; Fig. 2). E_{loc} was decreased and L_p was increased in the DS+ group compared to both the HC and DS- groups; C_p was decreased in the DS+ groups compared to the HCs; E_{glob} was decreased and λ was increased in the DS+ group compared to the HCs. No significant intergroup differences were found in other global network properties. In secondary analyses controlling for depression severity, conducted out of scientific interest and because the DS+ and DS- groups differed in depression severity, we confirmed that the DS+ group had decreased E_{glob} and E_{loc} and increased L_p levels compared to those of the DS- group. There was no significant difference between SAs and SPs in any of the global network properties.

Alterations in nodal brain network properties

Among the three groups, nodal efficiency differed ($p < 0.05$, Bonferroni correction) between the bilateral thalamus, bilateral caudate, bilateral supplementary motor area (SMA), left olfactory cortex, left medial orbitofrontal cortex (mOFC), right hippocampus, right medial superior frontal gyrus (mSFG), and right Rolandic operculum (ROL) (Table 2; Fig. 3). The DS+ group showed decreased nodal efficiency in the bilateral thalamus, left SMA, left olfactory cortex, left mOFC, right caudate and right hippocampus compared with both the DS- and HC groups. The DS- and DS+ groups both showed decreased nodal efficiency in the

left caudate compared to the HC group. The DS+ group showed decreased nodal efficiency in the right ROL, right mSFG and right SMA compared with the HC group. The DS- and DS+ groups showed a decreased nodal degree in the left caudate compared to the HC group (Table 2). After we controlled for the effects of depression severity, we found that the DS+ group had decreased depression severity, we found that the DS+ group had decreased nodal efficiency in the bilateral thalamus, left SMA, left olfactory cortex, left mOFC, right caudate and right hippocampus compared to the DS- group. There was no significant difference that survived Bonferroni correction at the $p < 0.05$ level between SAs and SPs in any nodal property.

Correlations of network alterations with symptom severity

Correlations between global metrics and clinical measures (HAMD and HAMA scores) were not significant, consistent with analyses indicating that differences between DS+ and DS- patients were not related to current symptom severity.

Discussion

Like those of healthy controls, the brain connectomes of MDD patients with and without suicide plans or attempts had a small-world architecture. However, E_{loc} was lower and L_p was greater in the DS+ group than in both the HC and DS- groups; C_p was lower in the DS+ group than in the HCs; E_{glob} was lower and λ was greater in the DS+ group than in the HCs group. Turning to nodal characteristics, decreased nodal efficiency was found in regions of fronto-limbic-basal ganglia-thalamic circuits, including the bilateral thalamus, left SMA, left olfactory cortex, left mOFC, right caudate and right hippocampus, in the DS+ group compared to both the HCs and DS- groups. The DS+ group showed decreased nodal efficiency in the right ROL, right mSFG and right SMA compared with the HC group. The DS- and DS+ groups showed decreased nodal efficiency

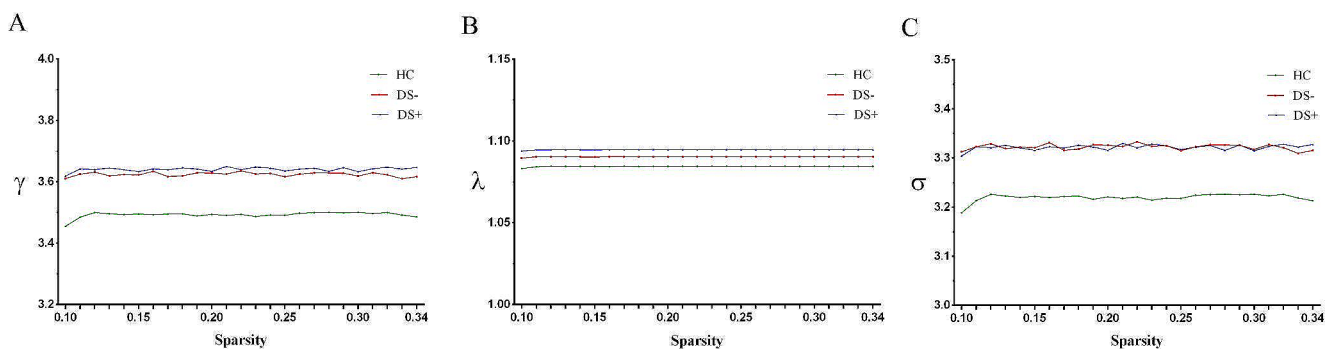


Fig. 1 All individuals exhibited the typical features of small-world topology: γ larger than 1 (A), λ approximately equal to 1 (B) and σ larger than 1 (C). Abbreviations γ : normalized clustering coefficient; λ : normalized characteristic path length; σ : small worldness

Table 2 Comparisons of regional network metrics for the HC, DS- and DS+ groups.

| | HC group | DS- group | DS+ group | p of ANOVA | p of Post-hoc Bonferroni correction | | | p value of t test ^a |
|-------------------------|-----------------|-----------------|-----------------|----------------------|-------------------------------------|---------------------|--------------------|--------------------------------|
| | | | | | HC vs. DS- | HC vs. DS+ | DS- vs. DS+ | |
| Global | | | | | | | | |
| C_p | 0.0622 ± 0.0048 | 0.0598 ± 0.0051 | 0.0593 ± 0.0061 | 0.0169 [*] | 0.104 | 0.019 [*] | 1 | 0.9313 |
| L_p | 1.2982 ± 0.0644 | 1.3256 ± 0.0947 | 1.3752 ± 0.1312 | 0.0006 [*] | 0.554 | <0.001 [*] | 0.045 [*] | 0.0363 [*] |
| λ | 0.2603 ± 0.0030 | 0.2617 ± 0.0031 | 0.2627 ± 0.0048 | 0.0054 [*] | 0.218 | 0.004 [*] | 0.521 | 0.1372 |
| E_{glob} | 0.0445 ± 0.0022 | 0.0437 ± 0.0030 | 0.0422 ± 0.0038 | 0.0011 [*] | 0.588 | 0.001 [*] | 0.066 | 0.0447 [*] |
| E_{loc} | 0.0622 ± 0.0037 | 0.0608 ± 0.0040 | 0.0584 ± 0.0054 | 0.0001 [*] | 0.434 | <0.001 [*] | 0.020 [*] | 0.0185 [*] |
| Nodal efficiency | | | | | | | | |
| Right ROL | 0.0397 ± 0.0037 | 0.0384 ± 0.0039 | 0.0366 ± 0.0041 | 0.0003 [*] | 0.298 | <0.001 [*] | 0.058 | 0.0585 |
| Left SMA | 0.0505 ± 0.0038 | 0.0490 ± 0.0042 | 0.0467 ± 0.0055 | 0.0001 [*] | 0.308 | <0.001 [*] | 0.037 [*] | 0.0430 [*] |
| Right SMA | 0.0487 ± 0.0039 | 0.0469 ± 0.0033 | 0.0454 ± 0.0043 | 0.0001 [*] | 0.069 | <0.001 [*] | 0.153 | 0.1985 |
| Left olfactory cortex | 0.0396 ± 0.0053 | 0.0390 ± 0.0053 | 0.0355 ± 0.0061 | 0.0004 [*] | 1 | 0.001 [*] | 0.006 [*] | 0.0039 [*] |
| Right mSFG | 0.0448 ± 0.0042 | 0.0428 ± 0.0045 | 0.0412 ± 0.0049 | 0.0005 [*] | 0.116 | <0.001 [*] | 0.225 | 0.0961 |
| Left mOFC | 0.0438 ± 0.0038 | 0.0435 ± 0.0044 | 0.0441 ± 0.0057 | 0.0003 [*] | 1 | 0.001 [*] | 0.003 [*] | 0.0086 [*] |
| Right hippocampus | 0.0471 ± 0.0052 | 0.0473 ± 0.0047 | 0.0434 ± 0.0060 | 0.0002 [*] | 1 | 0.001 [*] | 0.001 [*] | 0.0013 [*] |
| Left caudate | 0.0485 ± 0.0041 | 0.0453 ± 0.0044 | 0.0441 ± 0.0057 | <0.0001 [*] | 0.005 [*] | <0.001 [*] | 0.575 | 0.2144 |
| Right caudate | 0.0479 ± 0.0048 | 0.0462 ± 0.0046 | 0.0443 ± 0.0048 | 0.0005 [*] | 0.223 | <0.001 [*] | 0.120 | 0.0451 [*] |
| Left thalamus | 0.0515 ± 0.0035 | 0.0501 ± 0.0044 | 0.0479 ± 0.0046 | 0.0001 [*] | 0.321 | <0.001 [*] | 0.032 [*] | 0.0277 [*] |
| Right thalamus | 0.0503 ± 0.0034 | 0.0488 ± 0.0034 | 0.0460 ± 0.0053 | <0.0001 [*] | 0.216 | <0.001 [*] | 0.004 [*] | 0.0086 [*] |
| Nodal degree | | | | | | | | |
| Left caudate | 1.2013 ± 0.2823 | 0.9834 ± 0.2805 | 0.9883 ± 0.3207 | 0.0002 [*] | 0.001 [*] | 0.001 [*] | 1 | 0.2144 |

The data are shown as the mean ± SD. ^{*} indicates a significant difference between groups. The Bonferroni correction was applied to correct for multiple group comparisons of brain regions. All the brain region information was obtained via automated anatomical labeling (AAL).

Abbreviations HCs: healthy controls; DS-: patient with depression and no suicide plans or attempts; DS+: patient with depression and suicide plans or attempts; SD: standard deviation; C_p : clustering coefficient; L_p : path length; λ : normalized characteristic path length; ROL: Rolandic operculum; SMA: supplementary motor area; mSFG: medial superior frontal gyrus; mOFC: medial orbitofrontal cortex

^a Secondary analysis comparing both global and nodal properties between the DS+ and DS- groups using HAMD scores (minus suicide item) as a covariate

and nodal degree in the left caudate compared to the HC group. These findings expand the understanding of the neural mechanisms associated with suicide plans and attempts in MDD patients at the whole-brain connectome level.

Global topological alterations

Previous graph theory studies have demonstrated that the human brain is organized in a small-world network pattern, which reflects an optimal balance between segregation and network integration (Rubinov & Sporns, 2010; Sporns et al., 2005). Although the structural brain network of the DS+ group retained overall small-world architecture, it presented a decreased E_{glob} , E_{loc} and C_p and increased L_p and λ compared to those of the HCs, as well as a decreased E_{loc} and increased L_p compared to those of the DS- group.

E_{glob} is a measure of the efficiency of information exchange at the global level, and a decreased E_{glob} in our study suggested the impairment of the ability to combine information from distributed brain regions for depressed

suicidal patients (Latora & Marchiori, 2001). A short L_p and λ of the brain network ensure effective integrity and rapid information transmission between regions, forming the basis of optimal cognitive processes (Sporns & Zwi, 2004). The increased L_p and λ and decreased E_{glob} in suicidal patients compared to controls may contribute to the disrupted cognitive processes, inflexible behavioral preferences and impulsive behavior that have been associated with suicide risk. These alterations, including decreased E_{glob} and increased L_p , reflected weaker integration in DS+ patients than in HCs.

The E_{loc} measures the level of clustering, and a higher level of clustering is interpreted as a higher level of local organization in the network (Filippi et al., 2013). Therefore, the decreased E_{loc} in the suicidal group suggested a lower level of local connectedness and reduced network fault tolerance (Latora & Marchiori, 2001). The C_p , a network clustering coefficient, measures the cliquishness of a typical neighborhood (a local property). The decreased C_p in the suicidal depressed groups suggested that MDD patients

Fig. 2 Group differences in global topological properties among the HC, DS- and DS + groups. Abbreviations C_p : clustering coefficient; L_p : characteristic path length; γ : normalized clustering coefficient; λ : normalized characteristic path length; σ : small-worldness. An asterisk designates network metrics with significant group differences

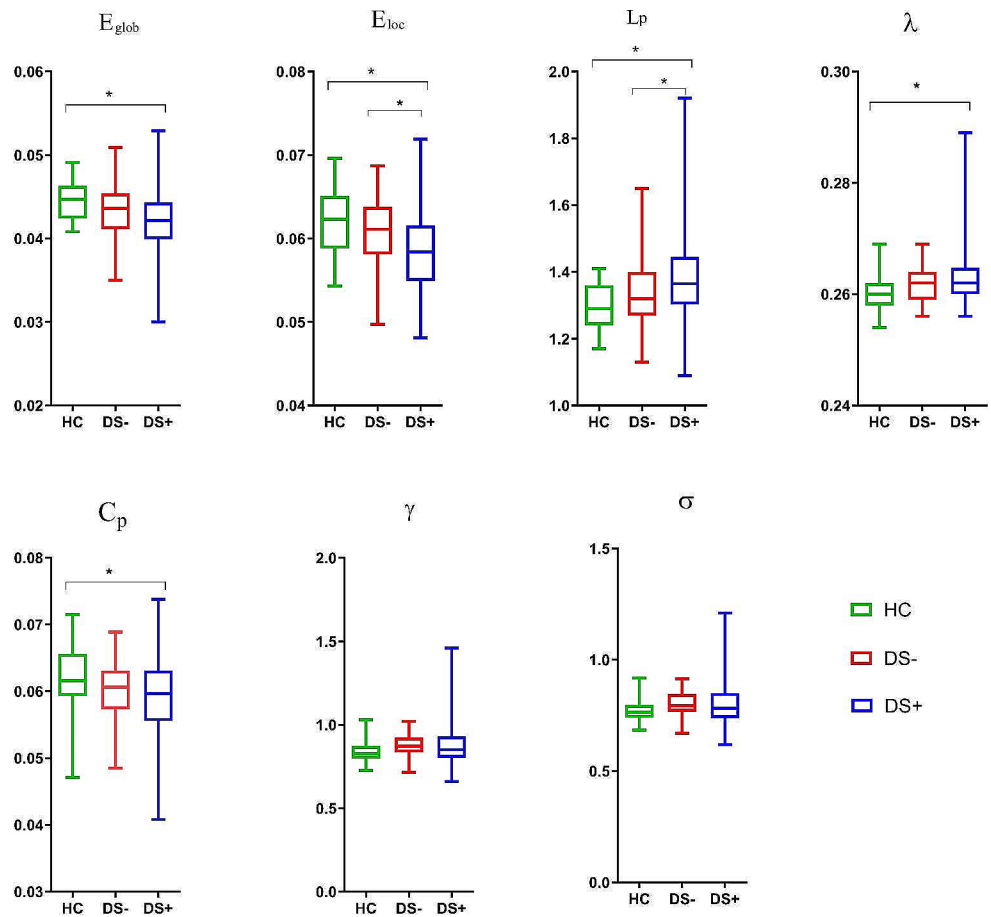
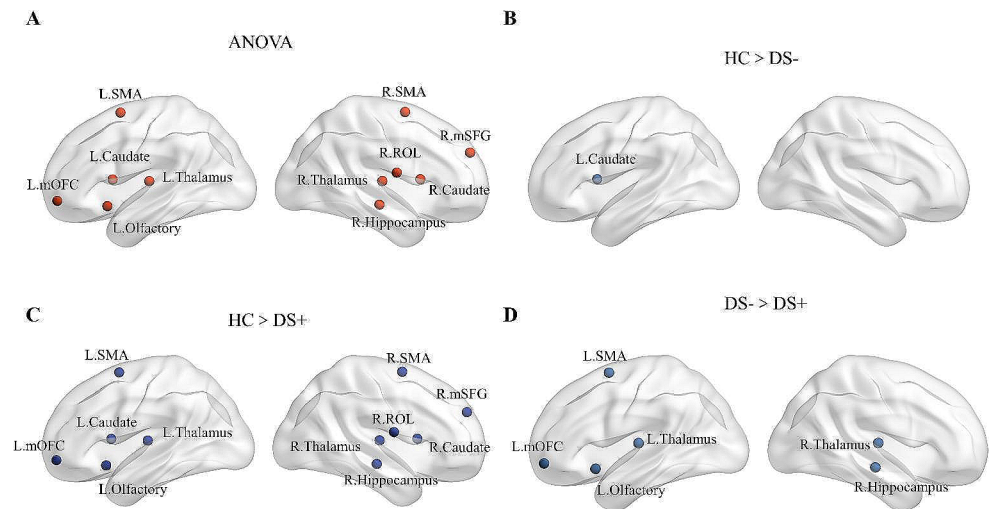


Fig. 3 Group differences in nodal efficiency among the HC, DS- and DS + groups.



with suicidality had a reduced density of local interconnectivity within brain networks compared to that in healthy controls (Rubinov & Sporns, 2010). Our findings suggested that those with suicide plans or attempts showed decreased segregation (reflected by decreased E_{loc} and C_p) of the brain anatomic connectome compared to that in both the DS and HC groups. This overall type of disrupted network organization (including both decreased integration and segregation)

has been reported previously in functional (Wang et al., 2016) and structural (J.-H. Chen et al., 2016; Li et al., 2017) network studies of MDD patients; however, notably, in the present study, the pattern was more pronounced in depressed patients at high risk for suicide.

Several previous studies using the graph theory framework to study the brain connectome in patients at risk for suicide reported somewhat different results: one study

reported that suicide attempters (Monkul et al.) had significantly greater integration (shorter L_p and greater E_{glob}) than suicidal ideation using diffusion tensor imaging (DTI)-based structural networks (Hwang et al., 2018), while another study reported increased integration (shorter L_p , λ and greater E_{glob}) in SAs compared to both patients and healthy controls using the functional brain network (Weng et al., 2019). Differences in the findings of these studies and the current study may be caused by differences in study samples. Our study compared depressed suicidal patients with non-suicidal depressed patients and healthy controls, while Hwang et al. (Hwang et al., 2018) compared suicide attempters with suicidal ideation and non-suicidal patients among veterans with more complex psychiatric comorbidities (mixed PTSD, mood disorders and substance dependence). The weaker small-worldness in our study may reflect an altered pattern of brain network organization more specifically related to suicide risk. Another reason for the small number of similar studies in this area is related to differences in imaging modalities and processing methods. For example, in our study, a structural network was constructed using diffusion tensor imaging (DTI), while Weng et al. (Weng et al., 2019) constructed a functional network using functional MRI. The application of multimodal imaging approaches for constructing brain networks may be beneficial in future connectome studies to comprehensively characterize network disturbances related to suicide risk.

Nodal topological alterations

Apart from global topological alterations, we also identified nodal topological alterations in the fronto-limbic-basal ganglia-thalamic circuitry in MDD patients with suicide plans or attempts not only relative to healthy controls but also to other depressed patients. These findings included decreased nodal efficiency in the bilateral thalamus, left mOFC, right hippocampus, left olfactory cortex and left SMA. The nodal degree is defined as the number of connections a node has with the rest of the network and is considered a measure of node interaction with the network, whereas nodal efficiency is the inverse of the harmonic mean of the shortest path length between a given node and all other nodes (Rubinov & Sporns, 2010). Our study revealed that, compared with those in the DS- group, almost all nodal-level alterations were decreased in efficiency but did not alter the nodal degree. This difference suggests that suicide-related alterations at the local level do not involve a reduced number of nodal connections but rather involve a longer average path length, suggesting that anatomic connectivity is less optimal for segregated and optimal information processing. The widespread alterations in nodal efficiency indicate longer path lengths of connections to these regions, consistent

with reduced segregation of network nodes, while the relative absence of alterations in nodal degree indicates a lack of actual reduction in the number of connections to these nodes.

Convergent evidence implicates impairments in the fronto-limbic brain circuitry that subserves emotion regulation and impulse control (Cox Lippard et al., 2014; Du et al., 2017; Johnston et al., 2017; Monkul et al., 2007). Decreased nodal efficiency in the fronto-limbic circuits in the suicidal group might have resulted in decreased information transmission efficiency. The caudate and thalamus both play crucial roles in working memory, decision-making and behavioral flexibility (Wei & Wang, 2016). Previous studies reported that depressed suicidal patients had a decreased caudate volume (Vang et al., 2010; Wagner et al., 2011) and decreased FA values in the thalamus (Jia et al., 2014), paralleling our current findings highlighting the relevance of alterations in these subcortical structures. In addition, a task-related fMRI study reported that suicide attempters showed decreased activation in the thalamus when making high-risk decisions but increased activation in the caudate when making low-risk decisions compared to controls (Pan et al., 2013). The medial OFC receives connections from the amygdala and thalamus and plays a crucial role in decision-making, especially when motivational and affective processes are more relevant (Dixon & Christoff, 2014). Together with the ventral striatum, these regions form core hubs of the reward network (Bracht et al., 2015). A study reported that reduced orbitofrontal-thalamic functional connectivity was negatively associated with the severity of suicidal ideation independent of depression severity (Kim et al., 2017). A decreased volume (Ding et al., 2015; Monkul et al., 2007), reduced thickness (Wagner et al., 2012) and decreased FA (Jia et al., 2014) in the OFC have also been reported previously in suicidal patients compared to controls. Early postmortem studies reported increased 5-hydroxytryptamine (5-HT) receptor binding in the PFC of the suicidal brain (Oquendo et al., 2006). Increased serotonin levels have been associated with high levels of impulsivity, which is a personality trait associated with suicide (Lopez-Castroman et al., 2014). Decreased nodal efficiency in the OFC was reported to be related to aggression and impulsivity. Previous studies also reported decreased low-frequency fluctuations (ALFF) (Cao et al., 2016) and hypoperfusion (Willeumier et al., 2011) in the limbic system and prefrontal cortex in suicidal patients compared to non-suicidal MDD patients. This pattern of findings in our study and previous work suggest alterations in regions and networks crucial for adaptive decision-making, including the OFC, striatum, and thalamus (Kim et al., 2017), which may be clinically relevant given recent meta-analysis findings confirming deficits

in decision-making in suicidal patients (Richard-Devantoy et al., 2014).

While a reduced volume of the olfactory cortex has been related to depression (Negoias et al., 2010; Rottstädt et al., 2018), alterations in the role of the olfactory cortex within the brain connectome (decreased nodal efficiency) in depressed suicidal patients were first reported in our study. The olfactory cortex has close functional and anatomical connections with emotion regulation networks, including the amygdala, insula, hippocampus, anterior cingulate cortex, and orbitofrontal cortex (Gottfried, 2006). We also found decreased nodal efficiency in the hippocampus in depressed suicidal patients compared to both comparison groups. The hippocampus is important for emotional recall and experience (Johnston et al., 2017). Previous studies have reported decreased hippocampal volumes in depressed suicidal patients compared to controls, consistent with regional pathology in this region, which might be related to alterations in white matter connectivity (Gosnell et al., 2016). Both the olfactory cortex and hippocampus are constituent parts of the limbic system that play crucial roles in emotional regulation and thus may be directly relevant for suicidal behavior. The decreased nodal efficiency in these areas suggested a potential mechanism for dysfunction of emotion regulation in depressed suicidal patients.

In the present study, we also found decreased nodal efficiency in the right ROL and left SMA in the DS+ group compared to the DS- group. A study reported decreased cerebral blood flow in suicide completers (Willeumier et al., 2011). The SMA is considered to constitute one of the neural regional networks that regulates the impact of negative emotion on behavioral planning (Ray & Zald, 2012). However, these areas may also influence brain networks in ways that disrupt planning, perception and communication to increase suicide risk.

Limitations

There are certain limitations in our current study. First, the DS+ group included both suicide attempters and planners, which may increase the sample heterogeneity of our DS+ group. We performed a nonparametric permutation test to compare SPs and SAs, which showed no significant differences between the two subgroups regarding either global or nodal topological parameters. Even so, the potential for differences between these groups merits future attention. Second, we cannot exclude the effects of medication because we included some patients who received medication, although medication status was matched between the two MDD patient groups (DS- and DS+). In addition, the DS- and DS+ groups were significantly but moderately different in terms of depression severity, which is a potential

confound for this study. While our secondary analyses (two-sample t test) comparing both global and nodal properties between the DS+ and DS- groups using HAMD scores (minus suicide item) as a covariate largely replicated our primary findings, this remains a consideration. Third, the DWI sequence used here had a relatively limited number of directions (40 total). In addition, we used deterministic fiber tractography to define the edges of the connectome, in which the tracking program can stop at fiber crossings. These limitations may decrease the precision of tract tracing. More directional DWI images or probabilistic tractography may be helpful for this purpose and are worthy of further study in the future. Fourth, the preprocessing workflow within PANDA corrected the image with no diffusion weighting ($b=0$) by calling the command ‘eddy correct’ in FSL 6.0.0, which limited us from using the new eddy methods in FSL. Finally, this was a cross-sectional study, and longitudinal studies are needed to investigate alterations in the white matter network over time and explore their role in the transition from suicidal intent to the completion of suicide.

Conclusion

In summary, this study demonstrated that the white matter structural network in the DS+ group exhibited weaker integration and decreased segregation than did that in both the DS- and HC groups. Decreased nodal efficiency was detected in the fronto-limbic-basal ganglia-thalamic circuit in the structural brain network of DS+ patients. This finding suggested an increased path length of fiber tracts connecting multiple nodes in the fronto-limbic-basal ganglia-thalamic circuitry, which may contribute to cognitive processing and impaired decision-making function in suicidal MDD patients. These results provide insights into the underlying neurobiology of suicide and suggest potential neuroimaging markers for identifying biomarkers for risk for suicide in MDD patients.

Supplementary Information The online version contains supplementary material available at <https://doi.org/10.1007/s11682-024-00870-1>.

Acknowledgements We thank all the participants including in this study.

Author contributions HRL contributed to the analysis and interpretation of data and drafting for the work. HWZ and HRL contributed to acquisition of imaging data. LY, HWZ and TLC contributed to acquisition of clinical scale data. KQ contributed to the analysis and interpretation of data. JAS, FFZ and ZQC revised it critically for important intellectual content. QYG and ZYJ contributed to the conception and design of the work, and made final approval for the version to be published. All authors approved the final version of the paper.

Funding This study was supported by the National Natural Science Foundation of China (82271947, 81971595, 81820108018 and 81621003), the CAMS Innovation Fund for Medical Sciences (CIFMS) (NO. 2022-I2M-C&T-B-104), the Key Program of Natural Science Foundation of Sichuan Province (2022NSFSC0047), the 1·3·5 Project for Disciplines of Excellence—Clinical Research Incubation Project, West China Hospital, Sichuan University (2020HXFH005), and the Key R&D Support Plan of Chengdu Science and Technology Bureau (Grant No. 2022-YF05-01766-SN).

Data availability Data supporting the results of this study can be obtained from the corresponding authors upon reasonable request.

Declarations

Ethical approval All procedures contributing to this work complied with the ethical standards of the relevant national and institutional committees on human experimentation and the Helsinki Declaration of 1975, as revised in 2008. The West China Hospital Clinical Trials and Biomedical Ethics Committee of Sichuan University approved our study protocol. All participants provided written informed consent.

Competing interests This manuscript has not been published and is not under consideration for publication elsewhere. We have no conflicts of interest to disclose. We do hope that the manuscript is suitable for your journal.

References

- Achard, S., & Bullmore, E. (2007). Efficiency and cost of economical brain functional networks. *Plos Computational Biology*, 3(2), e17. <https://doi.org/10.1371/journal.pcbi.0030017>.
- Arango, V., Underwood, M. D., & Mann, J. J. (2002). Serotonin brain circuits involved in major depression and suicide. *Progress in Brain Research*, 136, 443–453. [https://doi.org/10.1016/S0079-6123\(02\)36037-0](https://doi.org/10.1016/S0079-6123(02)36037-0).
- Arsenault-Lapierre, G., Kim, C., & Turecki, G. (2004). Psychiatric diagnoses in 3275 suicides: A meta-analysis. *Bmc Psychiatry*, 4, 37. <https://doi.org/10.1186/1471-244X-4-37>.
- Bracht, T., Linden, D., & Keedwell, P. (2015). A review of white matter microstructure alterations of pathways of the reward circuit in depression. *Journal of Affective Disorders*, 187, 45–53. <https://doi.org/10.1016/j.jad.2015.06.041>.
- Bullmore, E., & Sporns, O. (2009). Erratum: Complex brain networks: Graph theoretical analysis of structural and functional systems. *Nature Reviews Neuroscience*, 10(4), 312–312. <https://doi.org/10.1038/nrn2618>.
- Cao, J., Chen, X., Chen, J., Ai, M., Gan, Y., Wang, W., & Fang, W. (2016). Resting-state functional MRI of abnormal baseline brain activity in young depressed patients with and without suicidal behavior. *Journal of Affective Disorders*, 205, 252–263. <https://doi.org/10.1016/j.jad.2016.07.002>.
- Chase, H. W., Segreti, A. M., Keller, T. A., Cherkassky, V. L., Just, M. A., Pan, L. A., & Brent, D. A. (2017). Alterations of functional connectivity and intrinsic activity within the cingulate cortex of suicidal ideators. *Journal of Affective Disorders*, 212, 78–85. <https://doi.org/10.1016/j.jad.2017.01.013>.
- Chen, Z., Zhang, H., Jia, Z., Zhong, J., Huang, X., Du, M., & Gong, Q. (2015). Magnetization transfer imaging of suicidal patients with major depressive disorder. *Scientific Reports*, 5, 9670–9670. <https://doi.org/10.1038/srep09670>.
- Chen, J. H., Yao, Z. J., Qin, J. L., Yan, R., Hua, L. L., & Lu, Q. (2016). Aberrant Global and Regional Topological Organization of the fractional anisotropy-weighted brain structural networks in major depressive disorder. *Chinese Medical Journal*, 129(6), 679–689. <https://doi.org/10.4103/0366-6999.178002>.
- Colle, R., Chupin, M., Cury, C., Vandendrie, C., Gressier, F., Hardy, P., & Corruble, E. (2015). Depressed suicide attempters have smaller hippocampus than depressed patients without suicide attempts. *Journal of Psychiatric Research*, 61, 13–18. <https://doi.org/10.1016/j.jpsychires.2014.12.010>.
- Cox Lippard, E. T., Johnston, J. A. Y., & Blumberg, H. P. (2014). Neurobiological risk factors for suicide: Insights from Brain Imaging. *American Journal of Preventive Medicine*, 47(3, Supplement 2), S152–S162. <https://doi.org/10.1016/j.amepre.2014.06.009>.
- Ding, Y., Lawrence, N., Olie, E., Cyprien, F., le Bars, E., Bonafe, A., & Jollant, F. (2015). Prefrontal cortex markers of suicidal vulnerability in mood disorders: A model-based structural neuroimaging study with a translational perspective. *Transl Psychiatry*, 5, e516. <https://doi.org/10.1038/tp.2015.1>.
- Dixon, M. L., & Christoff, K. (2014). The lateral prefrontal cortex and complex value-based learning and decision making. *Neuroscience and Biobehavioral Reviews*, 45, 9–18. <https://doi.org/10.1016/j.neubiorev.2014.04.011>.
- Du, L., Zeng, J., Liu, H., Tang, D., Meng, H., Li, Y., & Fu, Y. (2017). Fronto-limbic disconnection in depressed patients with suicidal ideation: A resting-state functional connectivity study. *Journal of Affective Disorders*, 215, 213–217. <https://doi.org/10.1016/j.jad.2017.02.027>.
- Filippi, M., van den Heuvel, M. P., Fornito, A., He, Y., Pol, H., Agosta, H. E., & Rocca, F. M. A. (2013). Assessment of system dysfunction in the brain through MRI-based connectomics. *Lancet Neurology*, 12(12), 1189–1199. [https://doi.org/10.1016/S1474-4422\(13\)70144-3](https://doi.org/10.1016/S1474-4422(13)70144-3).
- Gosnell, S. N., Velasquez, K. M., Molfese, D. L., Molfese, P. J., Madan, A., Fowler, J. C., & Salas, R. (2016). Prefrontal cortex, temporal cortex, and hippocampus volume are affected in suicidal psychiatric patients. *Psychiatry Research: Neuroimaging*, 256, 50–56. <https://doi.org/10.1016/j.psychresns.2016.09.005>.
- Gottfried, J. A. (2006). Smell: Central nervous processing. *Advances in Oto-Rhino-Laryngology*, 63, 44–69. <https://doi.org/10.1159/000093750>.
- Hagmann, P., Cammoun, L., Gigandet, X., Meuli, R., Honey, C. J., Wedeen, V. J., & Sporns, O. (2008). Mapping the structural core of human cerebral cortex. *PLoS Biology*, 6(7), e159. <https://doi.org/10.1371/journal.pbio.0060159>.
- Hamilton, M. (1959). The assessment of anxiety states by rating. *British Journal of Medical Psychology*, 32(1), 50–55. <https://doi.org/10.1111/j.2044-8341.1959.tb00467.x>.
- Hamilton, M. (1960). A rating scale for depression. *Journal of Neurology, Neurosurgery and Psychiatry*, 23, 56–62. <https://doi.org/10.1136/jnnp.23.1.56>.
- Hawton, K., & van Heeringen, K. (2009). *Suicide Lancet*, 373(9672), 1372–1381. doi:[https://doi.org/10.1016/S0140-6736\(09\)60372-x](https://doi.org/10.1016/S0140-6736(09)60372-x).
- Honey, C. J., Sporns, O., Cammoun, L., Gigandet, X., Thiran, J. P., Meuli, R., & Hagmann, P. (2009). Predicting human resting-state functional connectivity from structural connectivity. *Proceedings of the National Academy of Sciences of the United States of America*, 106(6), 2035–2040. <https://doi.org/10.1073/pnas.0811168106>.
- Horiguchi, M., & Uno, H. (2020). On permutation tests for comparing restricted mean survival time with small sample from randomized trials. *Statistics in Medicine*, 39(20), 2655–2670. <https://doi.org/10.1002/sim.8565>.
- Hwang, J., Legarreta, M., Bueler, C. E., DiMuzio, J., McGlade, E., Lyoo, I. K., & Yurgelun-Todd, D. (2018). Increased efficiency of brain connectivity networks in veterans with suicide attempts. *NeuroImage Clinical*, 20, 318–326. <https://doi.org/10.1016/j.nicl.2018.04.021>.

- Jelescu, I. O., Zurek, M., Winters, K. V., Veraart, J., Rajaratnam, A., Kim, N. S., & Fieremans, E. (2016). In vivo quantification of demyelination and recovery using compartment-specific diffusion MRI metrics validated by electron microscopy. *Neuroimage*, *132*, 104–114. <https://doi.org/10.1016/j.neuroimage.2016.02.004>.
- Jenkinson, M., Beckmann, C. F., Behrens, T. E. J., Woolrich, M. W., & Smith, S. M. (2012). *FSL NeuroImage*, *62*(2), 782–790. doi:<https://doi.org/10.1016/j.neuroimage.2011.09.015>.
- Jia, Z., Huang, X., Wu, Q., Zhang, T., Lui, S., Zhang, J., & Gong, Q. (2010). High-field magnetic resonance imaging of suicidality in patients with major depressive disorder. *American Journal of Psychiatry*, *167*(11), 1381–1390. <https://doi.org/10.1176/appi.ajp.2010.09101513>.
- Jia, Z., Wang, Y., Huang, X., Kuang, W., Wu, Q., Lui, S., & Gong, Q. (2014). Impaired frontothalamic circuitry in suicidal patients with depression revealed by diffusion tensor imaging at 3.0 T. *Journal of Psychiatry and Neuroscience*, *39*(3), 170–177. <https://doi.org/10.1503/jpn.130023>.
- Johnston, J. A. Y., Wang, F., Liu, J., Blond, B. N., Wallace, A., Liu, J., & Blumberg, H. P. (2017). Multimodal Neuroimaging of Frontolimbic structure and function Associated with suicide attempts in adolescents and young adults with bipolar disorder. *American Journal of Psychiatry*, *174*(7), 667–675. <https://doi.org/10.1176/appi.ajp.2016.15050652>.
- Jung, J., Choi, S., Han, K. M., Kim, A., Kang, W., Paik, J. W., & Ham, B. J. (2020). Alterations in functional brain networks in depressed patients with a suicide attempt history. *Neuropsychopharmacology : Official Publication of the American College of Neuropsychopharmacology*, *45*(6), 964–974. <https://doi.org/10.1038/s41386-019-0560-z>.
- Kang, S. G., Na, K. S., Choi, J. W., Kim, J. H., Son, Y. D., & Lee, Y. J. (2017). Resting-state functional connectivity of the amygdala in suicide attempters with major depressive disorder. *Progress in Neuro-Psychopharmacology and Biological Psychiatry*, *77*, 222–227. <https://doi.org/10.1016/j.pnpbp.2017.04.029>.
- Kim, K., Kim, S. W., Myung, W., Han, C. E., Fava, M., Mischoulon, D., & Jeon, H. J. (2017). Reduced orbitofrontal-thalamic functional connectivity related to suicidal ideation in patients with major depressive disorder. *Scientific Reports*, *7*(1), 15772. <https://doi.org/10.1038/s41598-017-15926-0>.
- Latora, V., & Marchiori, M. (2001). Efficient behavior of small-world networks. *Physical Review Letters*, *87*(19), 198701. <https://doi.org/10.1103/PhysRevLett.87.198701>.
- Li, X., Steffens, D. C., Potter, G. G., Guo, H., Song, S., & Wang, L. (2017). Decreased between-hemisphere connectivity strength and network efficiency in geriatric depression. *Human Brain Mapping*, *38*(1), 53–67. <https://doi.org/10.1002/hbm.23343>.
- Li, L., Lei, D., Suo, X., Li, X., Yang, C., Yang, T., & Gong, Q. (2020). Brain structural connectome in relation to PRRT2 mutations in paroxysmal kinesigenic dyskinesia. *Human Brain Mapping*, *41*(14), 3855–3866. <https://doi.org/10.1002/hbm.25091>.
- Lopez-Castroman, J., Jausent, I., Beziat, S., Guillaume, S., Baca-Garcia, E., Genty, C., & Courtet, P. (2014). Increased severity of suicidal behavior in impulsive aggressive patients exposed to familial adversities. *Psychological Medicine*, *44*(14), 3059–3068. <https://doi.org/10.1017/s0033291714000646>.
- Monkul, E. S., Hatch, J. P., Nicoletti, M. A., Spence, S., Brambilla, P., Lacerda, A. L., & Soares, J. C. (2007). Fronto-limbic brain structures in suicidal and non-suicidal female patients with major depressive disorder. *Molecular Psychiatry*, *12*(4), 360–366. <https://doi.org/10.1038/sj.mp.4001919>.
- Mori, S., & van Zijl, P. C. (2002). Fiber tracking: Principles and strategies - a technical review. *NMR in Biomedicine*, *15*(7–8), 468–480. <https://doi.org/10.1002/nbm.781>.
- Mori, S., Crain, B. J., Chacko, V. P., & van Zijl, P. C. (1999). Three-dimensional tracking of axonal projections in the brain by magnetic resonance imaging. *Annals of Neurology*, *45*(2), 265–269. [https://doi.org/10.1002/1531-8249\(199902\)45:2<265::aid-ana21<3.0.co;2-3](https://doi.org/10.1002/1531-8249(199902)45:2<265::aid-ana21<3.0.co;2-3).
- Myung, W., Han, C. E., Fava, M., Mischoulon, D., Papakostas, G. I., Heo, J. Y., & Jeon, H. J. (2016). Reduced frontal-subcortical white matter connectivity in association with suicidal ideation in major depressive disorder. *Transl Psychiatry*, *6*(6), e835–e835. <https://doi.org/10.1038/tp.2016.110>.
- Negoias, S., Croy, I., Gerber, J., Puschmann, S., Petrowski, K., Joraschky, P., & Hummel, T. (2010). Reduced olfactory bulb volume and olfactory sensitivity in patients with acute major depression. *Neuroscience*, *169*(1), 415–421. <https://doi.org/10.1016/j.neuroscience.2010.05.012>.
- Olivet, D. M., Peruzzo, D., Thapa-Chhetry, B., Sublette, M. E., Sullivan, G. M., Oquendo, M. A., & Parsey, R. V. (2014). A diffusion tensor imaging study of suicide attempters. *Journal of Psychiatric Research*, *51*, 60–67. <https://doi.org/10.1016/j.jpsychires.2014.01.002>.
- Oquendo, M. A., Russo, S. A., Underwood, M. D., Kassir, S. A., Ellis, S. P., Mann, J. J., & Arango, V. (2006). Higher postmortem prefrontal 5-HT2A receptor binding correlates with lifetime aggression in suicide. *Biological Psychiatry*, *59*(3), 235–243. <https://doi.org/10.1016/j.biopsych.2005.06.037>.
- Pan, L., Segreti, A., Almeida, J., Jollant, F., Lawrence, N., Brent, D., & Phillips, M. (2013). Preserved hippocampal function during learning in the context of risk in adolescent suicide attempt. *Psychiatry Research*, *211*(2), 112–118. <https://doi.org/10.1016/j.psychres.2012.07.008>.
- Peng, H., Wu, K., Li, J., Qi, H., Guo, S., Chi, M., & Ning, Y. (2014). Increased suicide attempts in young depressed patients with abnormal temporal-parietal-limbic gray matter volume. *Journal of Affective Disorders*, *165*, 69–73. <https://doi.org/10.1016/j.jad.2014.04.046>.
- Ray, R. D., & Zald, D. H. (2012). Anatomical insights into the interaction of emotion and cognition in the prefrontal cortex. *Neuroscience and Biobehavioral Reviews*, *36*(1), 479–501. <https://doi.org/10.1016/j.neubiorev.2011.08.005>.
- Richard-Devantoy, S., Berlim, M. T., & Jollant, F. (2014). A meta-analysis of neuropsychological markers of vulnerability to suicidal behavior in mood disorders. *Psychological Medicine*, *44*(8), 1663–1673. <https://doi.org/10.1017/s0033291713002304>.
- Rottstädt, F., Han, P., Weidner, K., Schellong, J., Wolff-Stephan, S., Strauß, T., & Croy, I. (2018). Reduced olfactory bulb volume in depression—A structural moderator analysis. *Human Brain Mapping*, *39*(6), 2573–2582. <https://doi.org/10.1002/hbm.24024>.
- Rubinov, M., & Sporns, O. (2010). Complex network measures of brain connectivity: Uses and interpretations. *Neuroimage*, *52*(3), 1059–1069. <https://doi.org/10.1016/j.neuroimage.2009.10.003>.
- Sporns, O., & Zwi, J. D. (2004). The small world of the cerebral cortex. *Neuroinformatics*, *2*(2), 145–162. <https://doi.org/10.1385/ni:2:2:145>.
- Sporns, O., Tononi, G., & Kötter, R. (2005). The human connectome: A structural description of the human brain. *PLoS Computational Biology*, *1*(4), e42. <https://doi.org/10.1371/journal.pcbi.0010042>.
- Sui, J., Huster, R., Yu, Q., Segall, J. M., & Calhoun, V. D. (2014). Function–structure associations of the brain: Evidence from multimodal connectivity and covariance studies. *Neuroimage*, *102*, 11–23. <https://doi.org/10.1016/j.neuroimage.2013.09.044>.
- Suo, X., Lei, D., Chen, F., Wu, M., Li, L., Sun, L., & Gong, Q. (2017). Anatomic insights into disrupted small-world networks in Pediatric Posttraumatic stress disorder. *Radiology*, *282*(3), 826–834. <https://doi.org/10.1148/radiol.2016160907>.
- Suo, X., Lei, D., Li, L., Li, W., Dai, J., Wang, S., & Gong, Q. (2018). Psychoradiological patterns of small-world properties and a systematic review of connectome studies of patients with 6 major

- psychiatric disorders. *Journal of Psychiatry and Neuroscience*, 43(5), 170214. <https://doi.org/10.1503/jpn.170214>.
- Vanes, L. D., & Dolan, R. J. (2021). Transdiagnostic neuroimaging markers of psychiatric risk: A narrative review. *NeuroImage: Clinical*, 30, 102634. <https://doi.org/10.1016/j.nicl.2021.102634>.
- Vang, F. J., Ryding, E., Träskman-Bendz, L., van Westen, D., & Lindström, M. B. (2010). Size of basal ganglia in suicide attempters, and its association with temperament and serotonin transporter density. *Psychiatry Research*, 183(2), 177–179. <https://doi.org/10.1016/j.psychres.2010.05.007>.
- Wagner, G., Koch, K., Schachtzabel, C., Schultz, C. C., Sauer, H., & Schlösser, R. G. (2011). Structural brain alterations in patients with major depressive disorder and high risk for suicide: Evidence for a distinct neurobiological entity? *Neuroimage*, 54(2), 1607–1614. <https://doi.org/10.1016/j.neuroimage.2010.08.082>.
- Wagner, G., Schultz, C. C., Koch, K., Schachtzabel, C., Sauer, H., & Schlösser, R. G. (2012). Prefrontal cortical thickness in depressed patients with high-risk for suicidal behavior. *Journal of Psychiatric Research*, 46(11), 1449–1455. <https://doi.org/10.1016/j.jpsychires.2012.07.013>.
- Wang, Z., Yuan, Y., Bai, F., You, J., & Zhang, Z. (2016). Altered topological patterns of brain networks in remitted late-onset depression: A resting-state fMRI study. *Journal of Clinical Psychiatry*, 77(1), 123–130. <https://doi.org/10.4088/JCP.14m09344>.
- Wang, H., Zhu, R., Dai, Z., Tian, S., Shao, J., Wang, X., & Lu, Q. (2020). Aberrant functional connectivity and graph properties in bipolar II disorder with suicide attempts. *Journal of Affective Disorders*, 275, 202–209. <https://doi.org/10.1016/j.jad.2020.07.016>.
- Wei, W., & Wang, X. J. (2016). Inhibitory control in the Cortico-basal Ganglia-Thalamocortical Loop: Complex Regulation and Interplay with memory and decision processes. *Neuron*, 92(5), 1093–1105. <https://doi.org/10.1016/j.neuron.2016.10.031>.
- Weng, J. C., Chou, Y. S., Tsai, Y. H., Lee, C. T., Hsieh, M. H., & Chen, V. C. (2019). Connectome Analysis of Brain Functional Network Alterations in depressive patients with suicidal attempt. *J Clin Med*, 8(11). <https://doi.org/10.3390/jcm8111966>.
- Willeumier, K., Taylor, D. V., & Amen, D. G. (2011). Decreased cerebral blood flow in the limbic and prefrontal cortex using SPECT imaging in a cohort of completed suicides. *Transl Psychiatry*, 1(8), e28–e28. <https://doi.org/10.1038/tp.2011.28>.

Publisher's Note Springer Nature remains neutral with regard to jurisdictional claims in published maps and institutional affiliations.

Springer Nature or its licensor (e.g. a society or other partner) holds exclusive rights to this article under a publishing agreement with the author(s) or other rightsholder(s); author self-archiving of the accepted manuscript version of this article is solely governed by the terms of such publishing agreement and applicable law.